AXIAL

THE BEHAVIOR OF VARIANCE RESULTING FROM TURBULENT MIXING ZONE INTERACTION WITH SHOCKS

V.I. Kozlov, A.N. Razin
(RFNC – VNIIEF)

We have compared numerical and experimental data on turbulent mixing of two gases in a shock tube induced by Richtmeyer-Meshkov's instability. The calculations were performed with the 1D technique VIKHR. This technique implements Nikiforov's semi-empirical model. We compared both the mixing zones and the average variances of the velocity component parallel to the tube axis. There was no special algorithm for calculations of turbulent quantities at the shock front.

INTRODUCTION.

Nikiforov suggested the turbulent mixing model [1] to treat transient turbulent flows stipulated by Raleigh-Taylor and Richtmeyer-Meshkov instabilities. This model has been implemented in the difference form with the VIKHR technique [2]. Numerical simulations of various tests has shown that the model [1] provides satisfactory treatment of turbulent flows of multicomponent fluids without changing the model's constants [3÷5].

Basing on [3÷5] we can conclude that the information given by shock tube tests that only measure TM zone width as a function of time and the distribution of average density across this zone is incomplete. In fact, the width is an integral characteristic of the TM zone, and just this quantity taken alone is not sufficient to study in detail the interaction of the TM zone with shocks. On the other hand, TM models based on quite different principles can yield similar average density distributions without noticeable changes of TM zone width as a function of time. Still these model treat the TM zone "fine" structure (the distributions of turbulence intensity, turbulent energy dissipation rate, density fluctuations intensity, etc.) differently. If there is only one shock passing through the TM zone, the fine structure may have no considerable effects on the zone evolution (apparently, this accounts for the fact that different models yield similar results

for simple flows). Complex flows often have several TM zones that evolve simultaneously under the influence of multiple shocks, and different zones can join. More detailed information about TM zone structure and the mechanism of interaction with shocks is required for such flows.

New results in this direction have been obtained by French researchers in their tests [6]. These tests, which were arranged similarly to Meshkov's shock tube tests, were the first to systematically measure instantaneous flow velocities in the TM zone. The evolution of fluctuations of the axial mass flow velocity (the velocity component parallel to the tube axis) in the TM zone before and after it interacted with shocks reflected from the tube dead-end has been studied by means of Doppler's laser anemometry. Mean square fluctuations of the axial velocity have been calculated in five Eulerian points by statistical averaging of the multiple measurements.

This paper gives VIKHR numerical results on the experiments [6]. On the whole, there is good agreement with the experiments of both the TM zone width as a function of time and the axial variance $\overline{u_1'^2}$ as a function of time. Meanwhile, we must note that the calculation considerably overestimates (nearly twofold) the maximum $\overline{u_1'^2}$ when the TM zone interacts with the first shock reflected from the tube dead-end (this is the most intensive shock). In addition, the calculations have shown faster attenuation of $\overline{u_1'^2}$ with time compared to the experiments.

At present we are working on further development of the TM physical model implemented in the VIKHR technique. In particular, we are improving the correlations for turbulent transport and dissipative processes, and study the mechanism of TM zone interaction with shocks in more detail. The results calculated with the modified VIKHR will be presented upon completion of this work.

NUMERICAL RESULTS

The numerical domain of the problem is shown in the fig. 1. The initial gas pressure is equal to the atmospheric pressure of 1 bar. The initial air density is 0.0012 g/cm^3, that of SF_6 – 0.006 g/cm^3. Air and SF_6 were treated as perfect gases, the adiabatic index of air was $\gamma = 1.4$, that of SF_6 was $\gamma = 1.094$. The shock tube dead-end has

the co-ordinate 0 cm, the dead end being regarded as a rigid wall. The interface co-ordinate is 30 cm. At the right boundary (120 cm from the shock tube dead end) a constant pressure of 2.15 bar is set, which causes a shock in SF_6 with the front velocity of 197 m/s.

The comparison of the experimental data and the numerical data calculated with the VIKHR code is given in the fig. 2÷4. Note that $2e_1$ from VIKHR corresponds to the axial variance $\overline{u_1'^2}$.

The fig. 2 shows the R-t diagram of the TM zone boundaries. The start of the calculation is the reference time (the time when the shock reaches the interface is $t \approx 4.55$ ms), and the coordinate center is at the shock tube dead end (rigid wall). One can see that the experimental and numerical data are, on the whole, in satisfactory agreement. The R-t diagram of the finite-difference shock center calculated ~~with the algorithm [7]~~ is also given here. The fig. 2 shows that three shocks reflected from the dead end pass through the TM zone. In the calculation, however, only two waves can be regarded as shocks. As a matter of fact, an analysis of calculations with a sequence of refined grids has shown that the gas-dynamic gradients at the fronts of the first two waves are inversely proportional to the numerical point size, with much less pronounced dependence for the third wave. Thus, the third finite-difference wave can be regarded as a compression wave.

The fig. 3 shows the numerical (solid line) and experimental (step line) axial variance. The coordinates of the Eulerian points (transducers) where the velocity was measured, are given in mm from the initial interface location, and the time (ms) is counted from the moment when the shock reaches the interface.

The fig. 3 shows that before the first reflected shock enters the TM zone, the numerical and the experimental variance are in satisfactory agreement (according to the two transducers nearest to the interface: 51 mm and 125.5 mm). Note that when the TM zone passes through these ~~transducers~~, there are no shocks in the TM zone.

As for the third ~~transducer~~ (161 mm), the numerical variance is considerably higher than the experimental data. The fig. 2 shows that when the TM zone passes through this ~~transducer~~, the most intensive (the first) reflected shock is within the TM zone.

On the fourth transducer (169 mm) the numerical variance satisfactorily agrees with the experimental data. The fig. 2 shows that when the TM zone passes through this transducer, there are no shocks in the TM zone.

For the fifth transducer (178.5 mm) the numerical variance is lower than the experimental data, though the numerical data are close to the experimental data statistical scatter range. When the TM zone passes through this transducer two last reflected shocks are crossing the TM zone.

For the detailed analysis of the variance on the fifth transducer, numerical variance has been calculated as a function of time in three extra Eulerian points in the vicinity of the fifth transducer. The results are shown in the fig. 4 (the co-ordinates of the Eulerian points are counted from the dead-end).

According to the fig. 2, the left TM zone boundary (the one closer to the tube's dead-end) passes through the transducer with R = 12 cm earlier than it crosses the transducers with R = 11.5 cm and R = 11 cm. The second shock reflected from the rigid wall passes through the transducer with R = 12 cm later than it passes through those with R = 11.5 cm and R = 11 cm. It is shown in the fig. 4 as gradual increase of the signal recording time from R = 12 cm to R = 11 cm and decreasing maximum variance until the second reflected shock enters the TM zone. As the second shock, when it crosses the transducers, is in different Lagrangian points of the TM zone with different turbulence intensity, the peaks due to shock-TM zone interaction have different amplitudes at different transducers.

It is shown in the fig. 2 that the third reflected shock passes through the TM zone at 6.95 ms < t < 7.2 ms. In the fig. 4, one can see an increase of variance at the transducer with R = 11 cm during this time interval, while the other two transducers do not show any increase of the variance. The main reason for this is, apparently, that the third reflected shock (which is the weakest) interacts with the TM zone in Lagrangian points with different turbulence intensities, the turbulent intensity being the lowest at the transducers with R = 11.5 cm and R = 12 cm (the corresponding Lagrangian points are near the right boundary of the zone).

On the whole, we can state satisfactory agreement between the numerical results and experimental data, except for the transducer located at 161 mm from the shock tube

dead end. The numerical peak value for this ~~transducer~~ $2e_1$ is about 2 times higher than the experimental measurement $\overline{u_1'^2}$ (for the other ~~transducers~~ the numerical results are within the measurement uncertainty). Since when the TM zone passes through this ~~transducer,~~ the most intensive first reflected shock is in the TM zone, we can conclude that one of the reasons for this discrepancy can be that the model [1] unsatisfactorily describes the mechanism of shock-TM zone interaction. (As a matter of fact, the closure correlations of the model [1] have been developed for finite, rather small gas-dynamic gradients. Meanwhile, shocks in turbulent flows are discontinuity surfaces, like those in perfect fluids. This results from the fact that the minimum turbulent eddy size from the dissipative (Kolmogorov's) interval of spectrum is at least an order of magnitude higher than the interatomic distance).

REFERENCES.

1. *V.V.Nikiforov* Turbulent mixing at an interface of different-density fluids. // Voprosy Atomnoy Nauki i Techniki. Series: Theoretical and applied physics. 1985, issue 1, p. 3-8.

2. *V.A.Andronov, V.I.Kozlov, V.V.Nikiforov, A.N.Razin, Yu.A.Yudin* Turbulent mixing calcualtion technique for 1D flows (the VIKHR technique). // Voprosy Atomnoy Nauki i Techniki. Series: Mathematical modeling of physical processes. 1994, issue 2, s. 59-64.

3. *V.A.Andronov, S.M.Bakhrakh, E.E.Meshkov et.al.* An experimental study and numerical simulations of turbulent mixing in 1D flows // Doklady AN SSSR, 1982. vol. 264, № 1, p. 76-82.

4. *V.V.Nikiforov* Calculations of gravitational turbulent mixing in non-self-similar flows. // Voprosy Atomnoy Nauki i Techniki. Series: Theoretical and applied physics. 1993, issue 1, p. 3-12.

5. *V.V.Nikiforov, V.A.Andronov, A.N.Razin* Evolution of a turbulent mixing zone under shock impact // Doklady AN SSSR, 1995. vol. 343, № 3. p. 323-325.

6. ***Francoise Poggi, Marie-Helene Thorembey, Gerard Rodriguez.*** Velocity measurements in turbulent gaseous mixtures induced by Richtmyer-Meshkov instability. Physics of Fluids, v. 10, n. 11, 1998, pp. 2698-2700.

7. ***A.N.Razin*** An algorithm for finite-difference shock center location. // Voprosy Atomnoy Nauki i Techniki. Series: Theoretical and applied physics. 2001, issue 1, p. 43-50 .

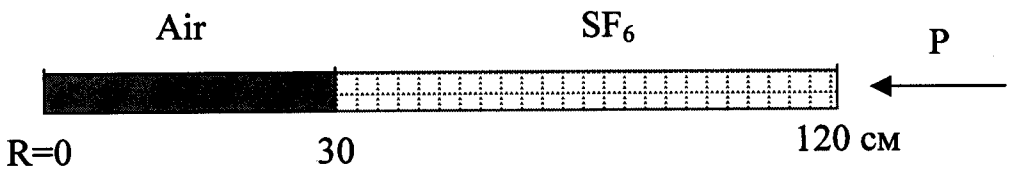

Fig. 1 Numerical geometry.

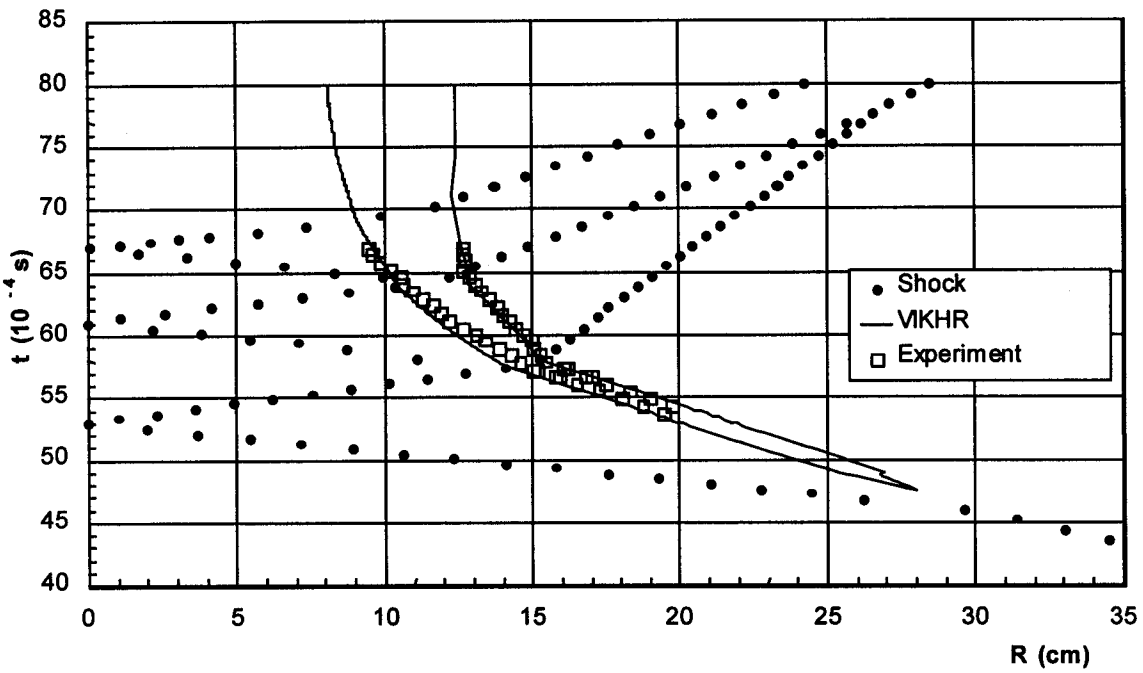

Fig. 2 R-t diagrams of the TM zone boundary and the shock

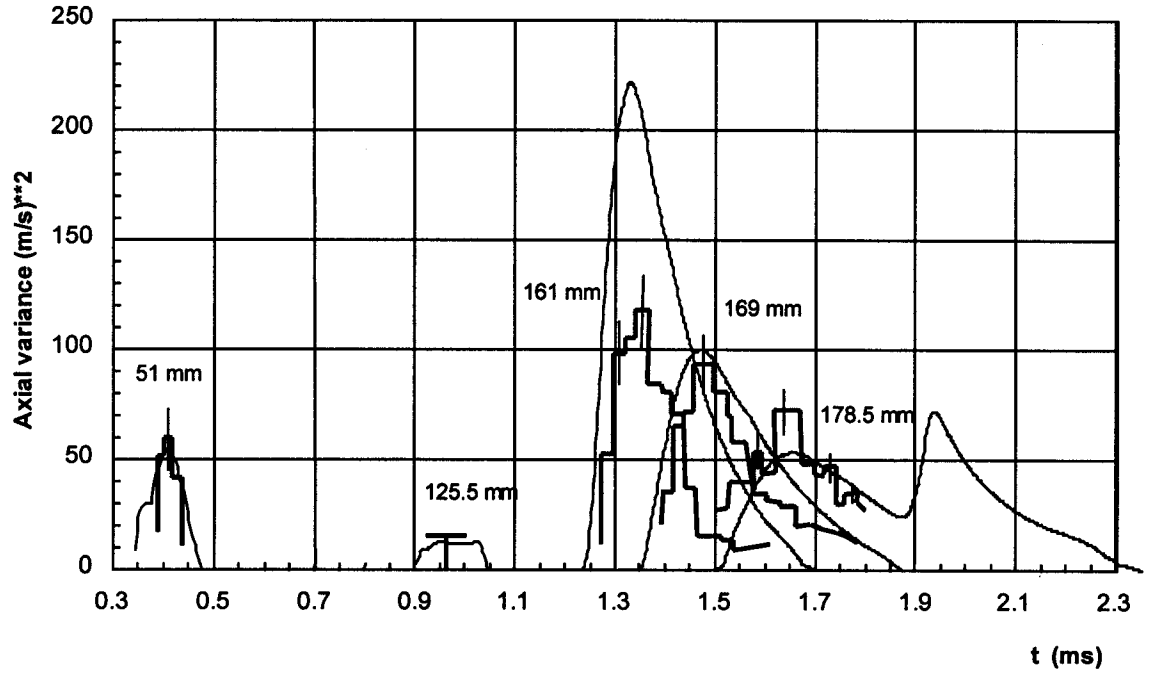

Fig. 3 Variance as a function of time given by different transducers

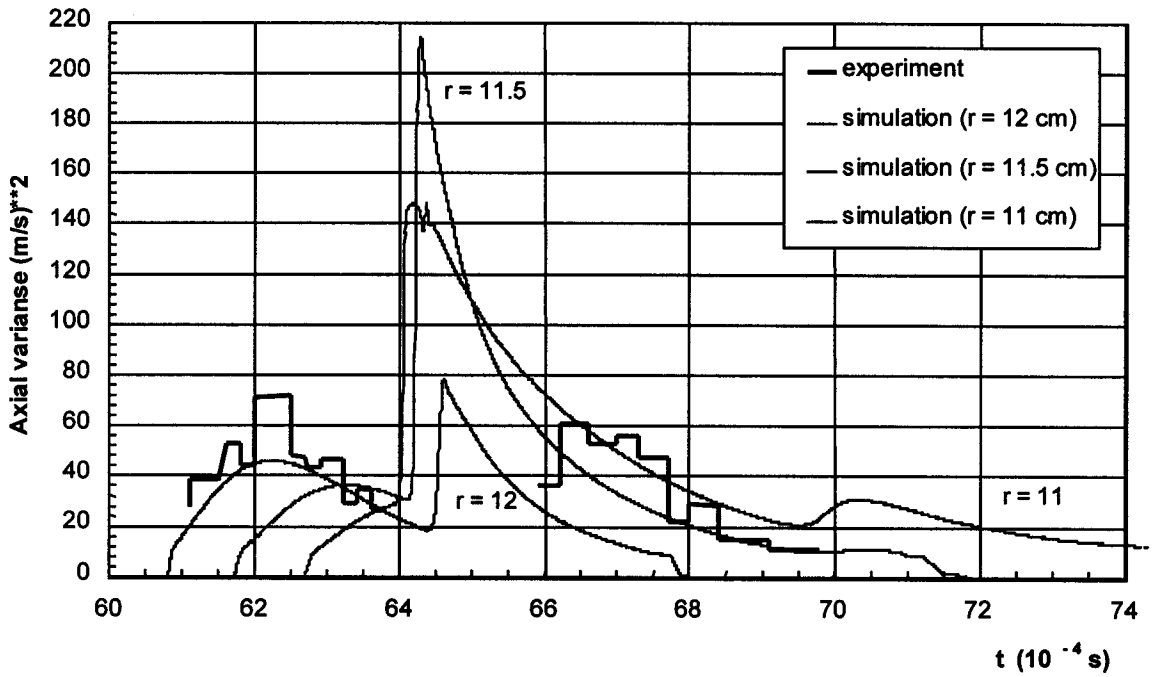

Fig. 4 Variance as a function of time in the vicinity of hte 5th transducer

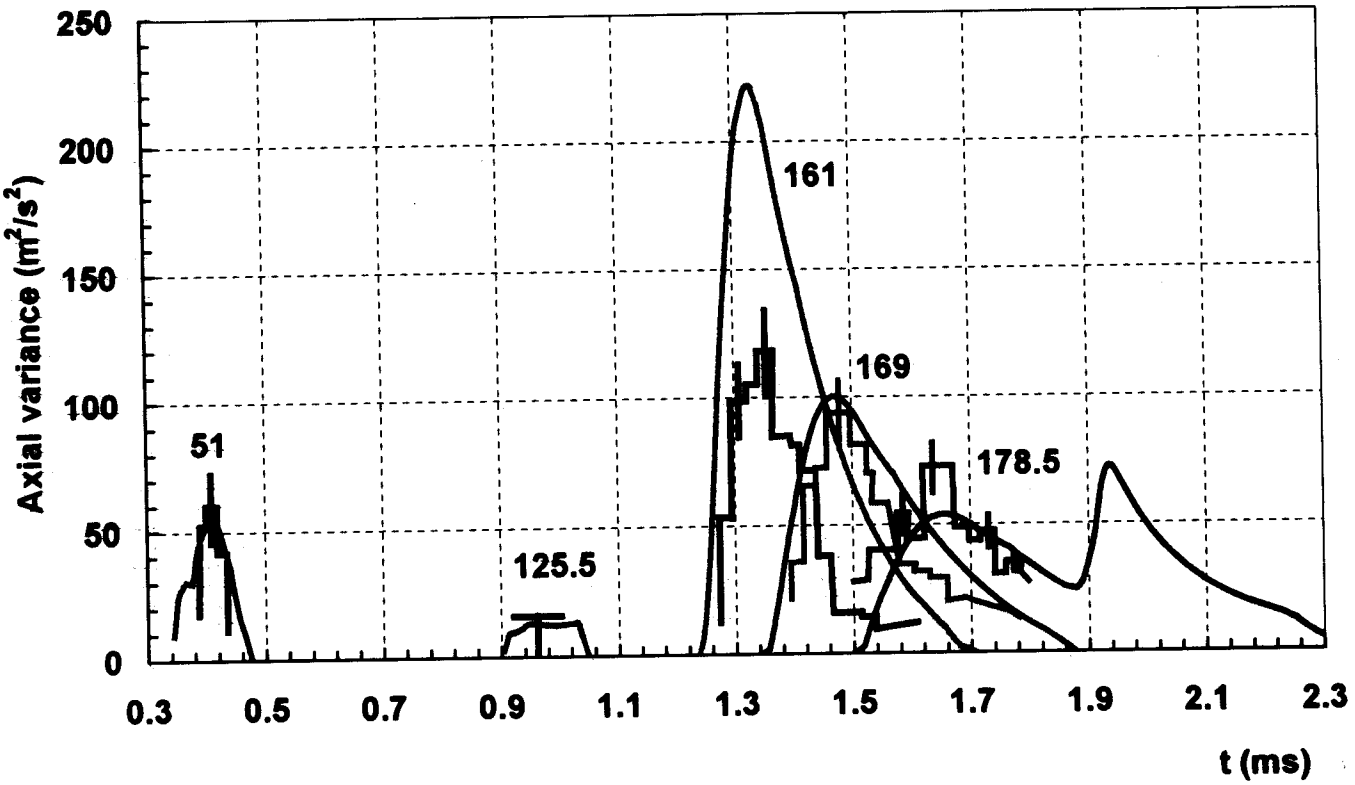

Fig. 3 Variance as a function of time given by different LDA probes.

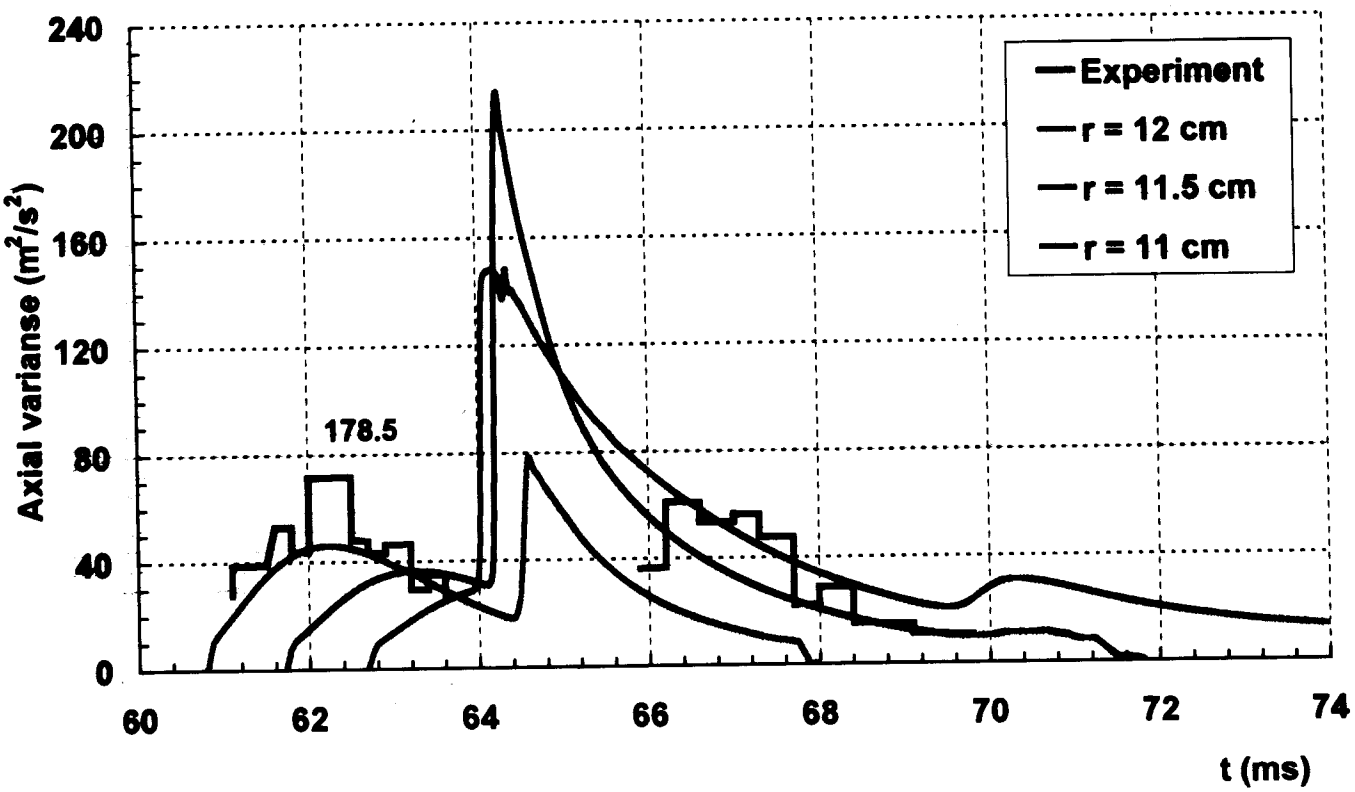

Fig. 4 Variance as a function of time in the vicinity of the 5th LDA probe.

NIKIFOROV'S MODEL OF TURBULENT MIXING (slab geometry)

$$\frac{d\rho}{dt}=-\rho\,\mathrm{div}U;\qquad \frac{dU}{dt}=-\frac{1}{\rho}\nabla\left(P+P_t\right);\qquad P_t=2\rho\frac{e_1}{e}\Phi;$$

$$\frac{dE}{dt}=-\frac{P}{\rho}\mathrm{div}\left(U-W\right)+\frac{1}{\rho}\mathrm{div}\left(\rho D\nabla E\right)+\frac{Q}{e}\Phi;\qquad \frac{dc_i}{dt}=\frac{1}{\rho}\mathrm{div}\left(\rho D\nabla c_i\right)$$

$$\frac{de_1}{dt}=\mathrm{div}\left(3D_t\nabla e_1-We_1\right)-e_1\mathrm{div}W-2V_{11}e_1+\left(1-\frac{\alpha k}{5}\right)f_1GW-\gamma\frac{Q}{e}\left(e_1-\frac{1}{3}e\right)-\frac{Q}{3};$$

$$\frac{de_2}{dt}=\mathrm{div}\left(D_t\nabla e_2-We_2\right)-e_2\mathrm{div}W+\frac{\alpha k}{10}f_1GW-\gamma\frac{Q}{e}\left(e_2-\frac{1}{3}e\right)-\frac{Q}{3};$$

$$\frac{d\Phi}{dt}=\frac{1}{\rho}\mathrm{div}\left[\rho\left(3D_t\nabla\Phi-W\Phi\right)\right]-2\frac{V_{11}e_1}{e}\Phi-W\frac{dU}{dt}-\frac{Q}{e}\Phi;$$

$$\frac{dQ}{dt}=\mathrm{div}\left(\frac{5}{3}D_t\nabla Q-WQ\right)-Q\mathrm{div}W-\frac{4}{3}\left(1+\frac{\gamma}{2}\frac{e_1-e_2}{e}\right)V_{11}Q+\frac{f_1GW}{3e_1}Q+$$

$$\beta\left(\frac{\alpha k}{5}f_1GW+\frac{2\gamma}{3}\frac{e_1-e_2}{e}Q\right)\frac{AW}{R}\left(1+R\right)-2\frac{Q^2}{ke};$$

$$\frac{dW}{dt}=\frac{1}{\rho}\mathrm{div}\left[\rho\left(2D_t\nabla W-W^2\right)\right]-V_{11}W+2Ae_1+f_1GR-k_1\frac{Q}{e}W;$$

$$\frac{dR}{dt}=\frac{1}{\rho^2}\mathrm{div}\left[\rho^2\left(D_t\nabla R-WR\right)\right]+R\mathrm{div}W+2AW-\frac{3}{2}\frac{Q}{e}R.$$

Here: $\nabla\equiv\frac{\partial}{\partial r};\quad \mathrm{div}\equiv\frac{\partial}{\partial r};\quad V_{11}=\frac{\partial}{\partial r}\left(U-W\right);\quad A=\frac{\nabla P}{\gamma_{ad}P}-\frac{\nabla\rho}{\rho};G=\frac{1}{\rho}\nabla P;$

$$e=e_1+2e_2;\qquad k=\frac{3e_2}{e}\sqrt{\frac{3e_1}{e}};\quad e_1=\overline{u_1'^2}/2;\qquad e_2=\overline{u_2'^2}/2;\qquad R=\overline{\rho'^2}/\rho^2;$$

$$W=\overline{\rho'u_1'}/\rho;\qquad \Phi=e+\overline{\rho'u_k'^2}/2\rho;\qquad f_1=\left(1+R-\frac{D_t}{W}\nabla R\right)^{-1}.$$

$$D=\begin{cases}W/A & if\ AW>0\\ 0 & f\ AW\le 0\end{cases};\qquad D_t=\frac{16\alpha_1e_1}{k_3+b};\qquad k_3=2\frac{Q}{e}\left(\gamma+\frac{e}{3e_1}+3\right);$$

$$b=\alpha_1\left(\xi+|\xi|\right);\quad \xi=\frac{2AW}{R}-k_2\frac{Q}{e}.$$

LDA probe positions from interface:

5.1 cm, 12.55 cm, 16.1 cm, 16.9 cm, 17.85 cm

Fig. 1 Numerical geometry.

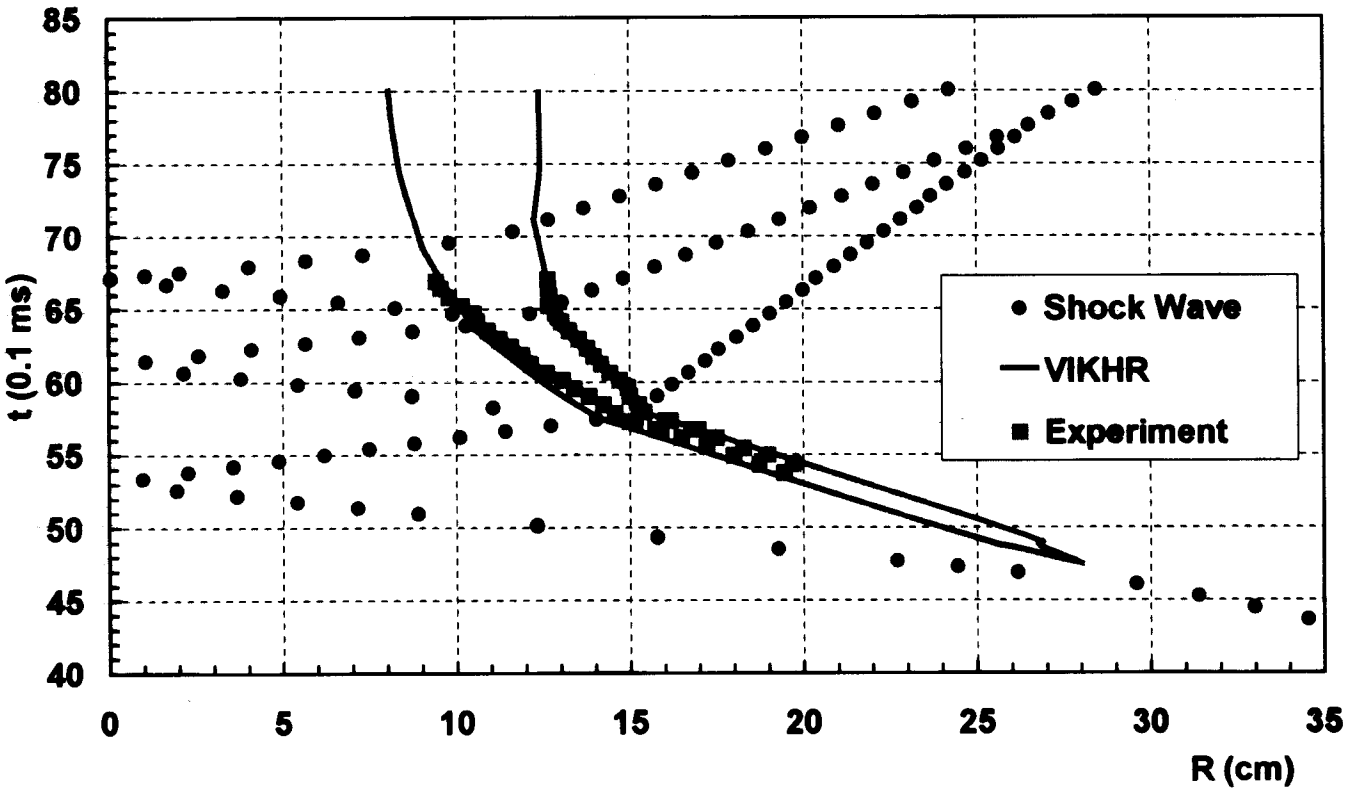

Fig. 2 R-t diagrams of the TM zone boundary and the shock